CHAPTER 2

LITERATURE REVIEW OF THEORETICAL BACKGROUND

Introduction

Optical fiber amplifiers have received increasing attention because of its important role in optical communication systems. Fibers can be made out of plastics, liquids and glasses, all of which can be doped, but the most suitable is glass since it offers a very low loss transmission medium which can be made in long lengths to give a continuous guiding medium. Section 2.1 provides a description of host glasses and dopants such as rare-earth ions in fiber. Elements that can be incorporated into the glass structure to give the important fluorescence properties necessary for some applications. The electronic energy level structure of three-level and four-level optical amplifier are generally analyzed and described in section 2.2. Section 2.3 outlines the amplification characteristics such as gain, amplified spontaneous emission(ASE), and noise in rare-earth doped fiber based on the steady-state rate equations and differential equations for the power change rates of the pump, signal, and ASE light propagated along a fiber in the guided mode. These features are of importance when constructing transmission systems that employ fiber amplifiers as in-line repeaters, booster amplifiers, and preamplifiers. This is because these amplification characteristics are used to analyze the maximum repeater spacing and the maximum number of available amplifiers in terms of data format, the SNR of an optical transmitter, receiver sensitivity, and transmission loss. Finally, model of an EYDFA that involves two energy levels of both Er^{3+} ion and Yb^{3+} ion is described in section 2.4.

2.1 Host Glasses and Rare-Earth Ions

By definition, glass is an inorganic product of fusion cooled to a rigid condition without crystallizing. The structural organization of glass is well defined at the scale of a few atoms, but is completely random, asymmetric and aperiodic at a larger scale. In general, when a liquid material is cooled down gradually, it will change to crystal, expelling the specific latent heat at a characteristic temperature, that is, the melting temperature. However, some special materials do not crystallize below the melting temperature and their viscosity increases to such a high value that they are solid with a disordered arrangement of atoms. Thus, a super cooled liquid is commonly called glass. Glass is in a state somewhere between that of a crystalline solid and a liquid.

The glass lattice is built from the basic structural units made of network former atoms. SiO_2, GeO_2, B_2O_3, P_2O_5, As_2O_3, and Sb_2O_3 are known as glass network formers. These network formers can form glass not only by themselves but also by mixing with other network formers in any mixing ratio. They are all capable of forming a three-dimensional network with O_2, thus providing the very strong covalent bonds that give glasses their characteristic properties. The conditions necessary for forming a glass with energy comparable to that of the crystalline form are as follows:

(i) an oxygen atom must not be linked to more than two atoms;

(ii) the number of oxygen atoms surrounding the network former atoms must be small:

(iii) the oxygen polyhedra must share corners with each other, not edges or faces:

(iv) at least three corners in each oxygen polyhedron must be shared.

Fig.1 displays two-dimensional structure analogies for (a) crystal silica and (b) silica glass. In reality, silicon atoms have one more bond with an oxygen atom and form a three-dimensional structure. The atomic arrangement of silica glass is thought to be a random arrangement of rigid oxygen tetrahedra (SiO_4^{-4}) that are formed based on the $Si\text{-}O_2$ covalent bonds. The atomic arrangement of silica glass in (b) is very similar to the crystalline form of silica (crystobalite) in (a), but the structure of silica glass in (b), being slightly more random, leads to the lack of long-range periodicity or symmetry. These random connections form a three-dimensional disordered lattice.

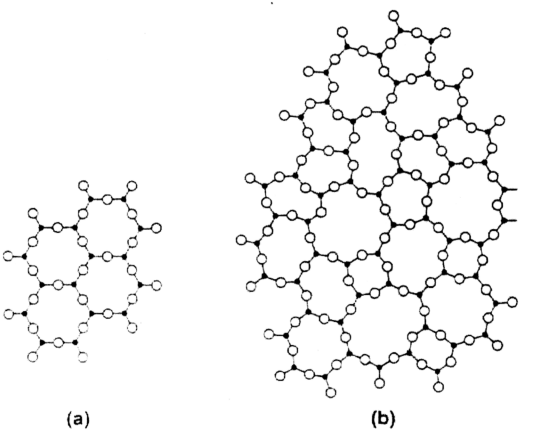

Fig.1(a) and (b) show the crystal silica and silica glass respectively, where the black dots indicate silicon atoms and the circles indicate oxygen atoms.

Other components, such as oxides of alkali metals and alkali-earth metals, can be added to the glass as network modifiers. Fig.2 shows that when these network modifier ions are added to the oxide glass, the $Si\text{-}O_2$ structure is opened up, weakening the bond strength, and lowering both the fusion temperature and the viscosity of the glass. The addition of network modifiers is important as it allows glass to be processed at workable temperature since pure silica requires very high temperatures for working.

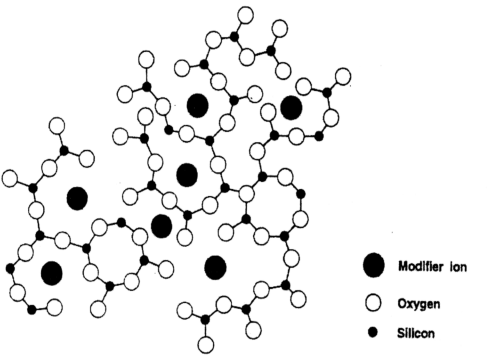

Fig.2 Schematic diagram of the silica glass matrix disrupted by the addition of network modifier ions.

Most transition metal oxides such as TiO_2, Al_2O_3, BeO, NiO, ZnO, and FeO in oxide glass introduce strong absorption in the visible and near-infrared wavelength region. Therefore, transition metals should be removed from the fiber materials in order to make low-loss optical fibers. Fluoride glasses, based on zirconium fluoride or hafnium fluoride as a network former, provide an interesting alternative to oxides glasses as a rare-earth ion host. Their lower

vibrational frequencies reduce intrinsic loss in the near-infrared region and enhance fluorescence properties for laser glass applications[1].

The different types of laser glasses can be grouped into four main categories: oxide, halide, oxyhalide, and chalcogenides. The advantages of glass as a laser host, compared to other solid-state material, such as crystalline, polycrystalline, or ceramic are: higher optical quality, transparency, low birefringence, high optical damage threshold, thermal shock resistance, weak refractive index nonlinearity, high energy storage and power extraction capacities, variety of possible composition, size and shape scalability, and low cost of raw materials. A general discussion of the merits of glass as host materials for laser ions is reported in [2].

A large variety of glasses are suitable as hosts for rare-earth ions such as Pr^{3+}, Nd^{3+} and Er^{3+}. Recently some interesting experimental work has also been done with dysprosium (Dy) since these ions require nonsilica host glasses in order to prevent phonon quenching of the fluorescence. A given rare-earth ion can relax from one energy level to a lower level by light emission or by non-radiative phonon emission. The nonradiative transitions occur by the emission of phonons. The phonons that are of importance are the highest energy phonons for the glass host in which the rare-earth is contained[3]. Table I show the typical values for the highest energy phonons in various glasses. The nonradiative transition probability W for emission between adjacent levels is given by

$$W = W_0 [\, 1 - \exp(-\frac{\hbar\omega}{kT})]^{\frac{\Delta E}{\hbar\omega}} \exp\{-\frac{\Delta E}{\hbar\omega}[\, \ln\frac{\Delta E}{\hbar\omega}\frac{1}{g} - 1]\}$$

where ΔE is the energy spacing between levels, $\hbar\omega$ is the highest energy phonon of the host glass and g is the electron-lattice coupling constant.

Table 1
Typical Values For The Highest Energy Phonon
$\hbar\omega$ (cm^{-1}) In Various Glasses

Glass	$\hbar\omega$
Borate	1350
Phosphate	1200
Silicate	1100
Germanate	900
Tellurite	700
Zblan	500
Chalcogenides	300

Fig.3 displays the periodic table designating the rare-earth series, main glass formers, main glass modifiers and intermediate elements. The rare-earth elements are a series of fifteen transition metals as shown in Table 2. All the elements have the configuration [1],[2],[3], $4s^2$, $4p^6$, $4d^{10}$, $4f^x$, $5s^2$, $5p^6$, $5d^y$ and $6s^2$ where [1],[2],[3] represent $1s^2$, $2s^2$, $2p^6$, $3s^2$, $3p^6$, $3d^{10}$ that are the closed shells for these levels, x=0 to 14 and y=0 or 1, but since the 4f level is an inner orbital, the effect of filling it has very little effect on the chemistry of the elements.

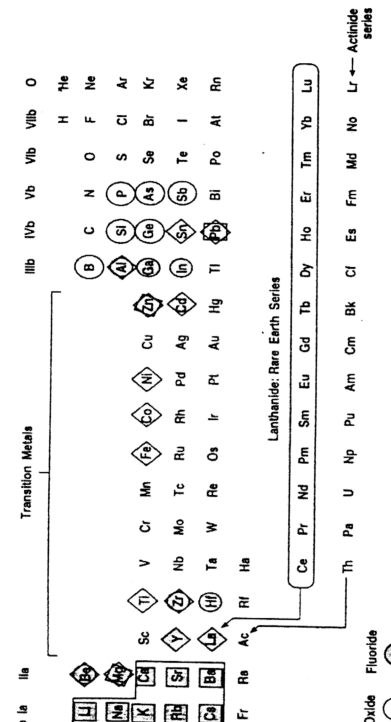

Fig.3 Periodic table designating rare-earth series, main formers, main glass modifiers, and intermediate elements.

Table 2

Structure and some properties of the rare-earth elements.

Element	Symbol	M	M^{3+}	Colour	Ionic radii / 10^{-10}m
Lanthanum	La	$5d^14f^0$	f^0	Colourless	1.060
Cerium	Ce	$5d^14f^1$	f^1	Pale yellow	1.034
Praseodymium	Pr	$5d^04f^2$	f^2	Green	1.013
Neodymium	Nd	$5d^04f^4$	f^3	Violet-pink	0.995
Promethium	Pm	$5d^04f^5$	f^4	—	—
Samarium	Sm	$5d^04f^6$	f^5	Colourless	0.964
Europium	Eu	$5d^04f^7$	f^6	Colourless	0.950
Gadolinium	Gd	$5d^14f^7$	f^7	Colourless	0.938
Terbium	Tb	$5d^04f^9$	f^8	Colourless	0.923
Dysprosium	Dy	$5d^04f^{10}$	f^9	Colourless	0.908
Holmium	Ho	$5d^04f^{11}$	f^{10}	Yellow	0.894
Erbium	Er	$5d^04f^{12}$	f^{11}	Pale pink	0.881
Thulium	Tm	$5d^04f^{13}$	f^{12}	Pale green	0.870
Ytterbium	Yb	$5d^04f^{14}$	f^{13}	Colourless	0.930
Lutetium	Lu	$5d^14f^{14}$	f^{14}	Colourless	0.850

The trivalent (3+) ionization preferentially removes two electrons from the 6s level and one electron from the 4f level. The electronic configuration for these ions is that of the xenon structure plus a certain number of 4f electrons. Thus, the electronic energy states of the rare-earth ions are determined by (i)the electronic configuration of the $4f^x$ level and also (ii)the effects of the environment on the $4f^x$ electrons, although such effects would not be strong. The observed infrared and visible optical spectra of trivalent rare-earth ions are a consequence of transitions between 4f states. In other words, the spectra of

the rare-earth compound is due to transitions of electrons between 4f energy levels. The metastable level in the rare-earth ion is always well separated from the lower levels, making nonradiative transitions difficult and so fluorescence is observed between these levels.

The ionic radii of the trivalent ions reduce very slightly down the series as shown in Table 2, except for ytterbium. The ionic radii are large and the field strength is low for rare-earth ions if compared to the first row transition elements, where the ionic radii are much smaller and more variable throughout the series since the valency of the most stable ion changes from M^{2+} through to M^{4+}. The rare-earth ions are not significantly affected by the ligand because the valency electrons are well shielded from outside influences. In contrast, the transition metal ions are greatly influenced by their environment because the valence electrons are not as well shielded by the outer orbitals from the environmental effects.

In general, the glass host composition impacts significantly the solubility of the rare-earth dopant which in turn affects the fluorescence lifetime and fluorescence line shape. Besides, the excited state absorption (ESA) can also be substantially affected by the choice of host glass compositions. This ESA phenomenon can seriously diminish the efficiency of an active fiber device.

2.2 General Concepts of Three- and Four-level Optical Amplifier System

Optical amplifiers amplify incident light through stimulated emission. Its main ingredient is the optical gain realized when the amplifier is pumped to achieve population inversion. Depending on the energy levels of the dopant, three-level laser transitions (e.g., the $^4I_{13/2}$ to $^4I_{15/2}$ transition of Er^{3+} in SiO_2) and four-level laser transitions (e.g., the $^4F_{3/2}$ to $^4I_{11/2}$ transition of Nd^{3+} in SiO_2) can be modeled according to the simplified energy diagram of Fig.4(a) and (b), respectively.

In both cases, ground state absorption (GSA) occurs between levels 1 and 3, followed by a rapid decay to the upper laser level 2. The stored energy in levels 2 is used to amplify a signal beam through stimulated emission. When pump ESA is present in a three-level laser system, pump absorption also takes place between levels 2 and 4, with a rapid relaxation from 4 back to 2 via primarily multi-phonon interactions. In a four-level laser system, the lower laser state has an energy level higher than the ground state, and is not populated. The main difference between the three- and four-level pumping schemes is related to the energy state occupied by the dopant after each stimulated emission event. In the case of a three-level scheme, the ion ends up in the gound state, whereas it remains in an excited state in the case of four-level pumping scheme. Besides, in a three-level system, the lower laser level coincides with the gound state, which leads to the existence of the pump threshold whereas in a four-level system, there is no pump threshold. Therefore, a three-level system must be designed properly to limit reabsorption of the signal due to the presence of ground state reabsorption at the signal

wavelength. This event does not happen to a four-level system as it does not have ground-state signal reabsorption which can degrade the performance of amplifier[4,5].

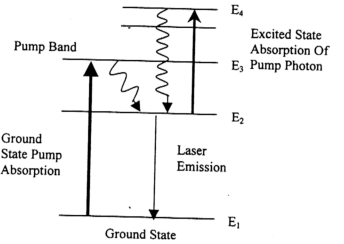

(a)

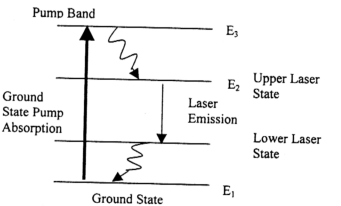

(b)

Fig.4. Simplified energy states of (a) a three-level laser with ESA at the pump wavelength, and (b) a four-level laser.

An important parameter to differentiate both systems is the ratio of the signal absorption rate to the signal emission rate. This ratio is unity for an ideal three-level laser and zero for a four-level laser. However, in Er:SiO_2 fiber, the $^4I_{13/2}$ and $^4I_{15/2}$ levels are Stark-split manifolds in thermal equilibrium and the ratio is generally different from unity and wavelength dependent. Er:SiO_2 fiber lasers have thus been shown to behave like four-level laser at long wavelengths[6].

2.3 Amplification Characteristics of an Optical Amplifier

The basic characteristics of an optical amplifier are shown in Fig.5. The incident optical signal is amplified after traversing the optical amplifier. In addition to signal amplification in the forward direction, the amplifier also includes other optical powers to the optical network. These added optical powers, which travel in both directions of the optical fiber, are: (i) Amplified spontaneous emission(ASE), (ii) Excess power from the pump laser, and (iii) Time-delayed scaled-replicas of the signal power.

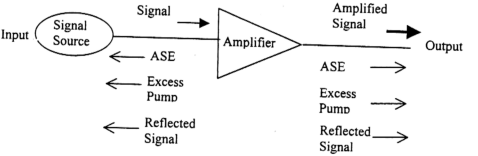

Fig. 5 Signal amplification of an optical amplifier.

An amplifier performance is actually limited by several physical effects and device constraints. The most fundamental limitation is due to the energy conservation principle: the maximum signal energy that can be extracted from a fiber amplifier cannot exceed the pump energy that is stored in it[7]. This principle of energy conservation can be expressed in terms of photon flux, that is,

$$\phi_s^{out} \le \phi_p^{in} + \phi_s^{in} \tag{2.1}$$

where $\phi_p^{in} = \frac{P_p^{in}}{h\upsilon_p}$ is the flux of pump photons input to the amplifier, and

$\phi_s^{in,out} = \frac{P_s^{in,out}}{h\upsilon_s}$ is the flux of signal photons input or output from the amplifier.

The inequality in this equation implies several possible effects:

(1) some pump photons can be lost due to various causes such as background or impurity loss,

(2) some pump photons can traverse the amplifier without interacting with the active ions,

(3) some pump photons which are absorbed by the active ions are lost by spontaneous emission, not converted into signal energy.

2.3.1 Gain Characteristics

Gain is the most fundamental parameter of an optical amplifier. For an amplifier free from spontaneous emission, gain, G is described as the ratio of the optical signal power in a fundamental mode radiated into free-space from the specified output fiber to a similar type of power from the input fiber

specified. This gain is defined for a single spatial or polarization mode since different modes may exhibit different gains. It is written as

$$G = \frac{P_s^{out}}{P_s^{in}} \tag{2.2}$$

Equation (2.2) can also be expressed in terms of input/output powers. From equation (2.1),

$$P_s^{out} \le P_s^{in} + \frac{\lambda_p}{\lambda_s} P_p^{in} \tag{2.3}$$

Thus,

$$G \le 1 + \frac{\lambda_p}{\lambda_s} \frac{P_p^{in}}{P_s^{in}} = 1 + \frac{\phi_p^{in}}{\phi_s^{in}} \tag{2.4}$$

From equation (2.4), it shows that the upper limit for the gain corresponds approximately to the flux ratio $\frac{\phi_p^{in}}{\phi_s^{in}}$. It implies that the maximum possible amplifier gain corresponds to the case where each pump photon is converted into one signal photon and this can be reached only if all pump photons are actually absorbed by the amplifying medium. However, in actual amplifier, the finite number of rare-earth ions existing in the medium limits the absorption of pump photons.

Ideally, an optical amplifier would amplify the input signal by its gain and produce no additional output. However, an optical amplifier also produces ASE, which adds to the spontaneous emission produced by the source. Thus, the optical amplifier gain, G is defined as

$$G = \frac{P_s^{out} - P_{ASE}}{P_s^{in}} \tag{2.5}$$

where P_s^{in}, P_s^{out} are the amplifier input and output signal powers respectively and P_{ASE} is the noise power generated by the amplifier which lies within the optical bandwidth of the measurement.

An understanding of the net amplifier gain can be derived from an analysis of the gain from individual "slice" along the fiber. An ASE-free two-level approximation is assumed[8]. An optical amplifier is actually a concatenation of many amplifiers of incremental length, Δz. Gain is composed of the contribution of all the gain elements, g(z) along the amplifier fiber as shown in Fig.6.

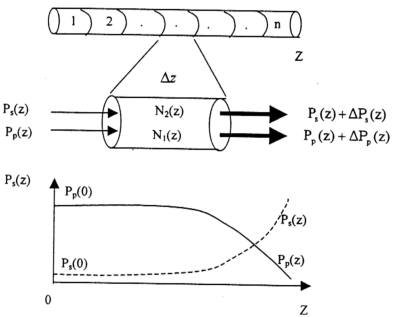

Fig.6 A simplified ASE-free two-level optical amplifier. Graph above shows the pump absorption and signal amplification along the active fiber.

The incremental signal gain, g(z) for a photon propagating down the fiber is dependent on the metastable state population density,N_2, the ground

state population density,N_1, the stimulated emission cross-section, σ_e, the absorption cross-section, σ_a, and the confinement overlap integrals factor, Γ_s, between the signal field and the active rare-earth ion population[7]. Both emission and absorption cross-sections represent the strength of the transition or the ability to produce gain or absorption respectively. The net gain, G, at the output fiber:

$$G = \lim_{\Delta z \to 0} \left\{ e^{g(z_1)\Delta z} \mathrm{x} e^{g(z_2)\Delta z} \mathrm{x} \ldots e^{g(z_n = L)\Delta z} \right\} = \exp\left(\int_0^L g(z) dz \right) \tag{2.6}$$

where $g(z)$, the gain element, is given as

$$g(z) = \Gamma_s \left[\sigma_{e,s} N_2(z) - \sigma_{a,s} N_1(z) \right] \tag{2.7}$$

also, the pump loss in a slice of fiber is given as

$$\alpha_p(z) = \Gamma_p \left[\sigma_{e,p} N_2(z) - \sigma_{a,p} N_1(z) \right] \tag{2.8}$$

When the pump light and signal light propagate in the same direction along the fiber and ASE is negligible (low gain approximation), the changes in pump and signal powers after propagation through a slice of doped fiber are:

$$\frac{dP_s}{dz} = g(z) P_s(z) \tag{2.9}$$

$$\frac{dP_p}{dz} = \alpha_p(z) P_p(z) \tag{2.10}$$

As the magnitude of the signal increases along the fiber, the upper-state population is reduced and this results in increased pump absorption in the increment of fiber.

From Equation (2.6) and (2.7), the net amplifier gain is found to be:

$$G = \exp\{\Gamma_s [\sigma_e [N_2] - \sigma_a [N_1]] L\} \tag{2.11}$$

In an optical amplifier, the effective input noise, $P_{noise,eff}$ will be multiplied by the amplifier gain and yields the output noise power of the amplifier. However, if the input power is small compared to $P_{noise,eff}$, its effect on the amplifier will be insignificant and the amplifier will be in small signal operation. In this small-signal gain region which correspons to input power levels, the signal amplification or the amplifier's gain does not reduce. If an optical amplifier is operated at large input signal level, it will cause saturation of the amplifier gain where there is a reduction in gain with an increase in signal power.

In the gain saturation region, the gain in an ASE-free amplifier model can be written as a function of the ratio of the output power to the saturation power.

$$G = G_0 \exp\left[-\frac{G-1}{G}\frac{P_s^{out}}{P_{sat}}\right] \tag{2.12}$$

where G_0 is the small-signal gain, P_{sat} is the saturation power at a specific wavelength , which is required to invert a slice of fiber sufficiently to obtain optical transparency (i.e. G=0) and it is written as

$$P_{sat} = \frac{Ah\upsilon}{\sigma_a \tau_{sp}} \tag{2.13}$$

where A is the mode-field area, σ_a is the absorption cross-section, and τ_{sp} is the spontaneous lifetime of the ion in the metastable state.

2.3.2 Amplified Spontaneous Emission (ASE) & Excited State Absorption (ESA)

The generation of noise in optical amplifier is an effect of the spontaneous deexcitation of the laser ions. With a finite excited state lifetime, some of the ions spontaneously return to the ground state, thereby emitting photons. These photons have no coherence characteristics with respect to the incoming signal light. In other words, this spontaneous emission has a random phase and direction. Typically less than 1% of the spontaneous emission is captured by the optical fiber mode and travels in both directions along the length of the active fiber. These photons are subsequently amplified in the same way as the signal, and result in amplified spontaneous emission (ASE). Once in the ground state, absorption of a pump photon activates the rare-earth ion again and the process repeats itself. It forms a background noise adding to the amplified signal. Thus, the presence of ASE causes degradation of the signal to noise ratio (SNR) of signals passing through the amplifier.

The rate of spontaneous emission power in bandwidth $d\upsilon$, is written as

$$\frac{dP_{SE}^{\cdot}}{dz} = 2P_0\sigma_e(\upsilon)\int N_2(r,\theta)\Psi_s(r,\theta)rdrd\theta \tag{2.14}$$

where $P_0 = h\upsilon\partial\upsilon$ is the power of one spontaneous noise photon in bandwidth $\partial\upsilon$ or referred to as equivalent input noise. The factor of 2 implies the spontaneous emission in both polarization modes of the fiber.

Another process that affects amplification is excited state absorption (ESA). ESA has long been acknowledged as a potential problem in laser system[9]. Absorption of the pump radiation by the upper laser level (pump ESA) lowers the overall efficiency of an amplifier and increases heating in the

gain medium. This pump ESA happens only if the ESA cross section overlaps with the GSA or pump cross section. Absorption of the laser radiation by the upper laser level (signal ESA) reduces the maximum gain. The effect of ESA can occur from any energy level having finite atomic population. Fig.7 shows an energy level diagram of Er:Silica glass with several possible GSA and ESA transitions and associated wavelengths.

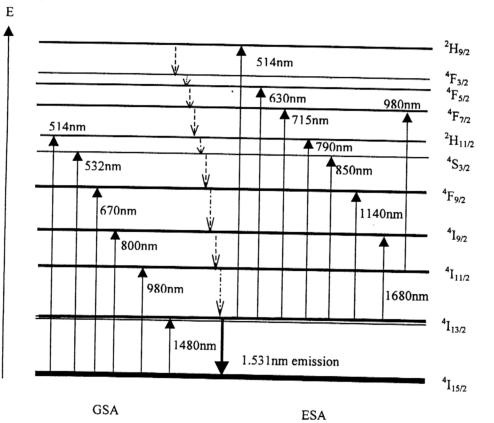

Fig. 7 GSA and ESA transitions with corresponding peak wavelengths in Er:Silica glass[7].

The ESA absorption cross section (σ_{ESA}) with respect to the GSA absorption cross section (σ_{GSA}) are important parameters since they affect the

pump or signal ESA at a given pump wavelength. The ESA and GSA absorption cross section ratio, δ, is given as

$$\delta = \frac{\sigma_{ESA}(\lambda_p)}{\sigma_{GSA}(\lambda_p)} = \frac{\alpha_{ESA}(\lambda_p)}{\alpha_{GSA}(\lambda_p)} \tag{2.15}$$

where α_{ESA} and α_{GSA} is the corresponding ESA and GSA absorption coefficients respectively. α_{ESA} and α_{GSA} in the wavelength range of 420-850nm of EDF had been measured and reported in [10].

This parameter δ is host glass composition dependent and it is attributed to two factors:

(i) the shift in peak wavelength of the GSA and ESA transitions relative to each other, which reflects changes in the Stark level positions.

(ii) the changes in peak cross sections for both GSA and ESA absorption.

In the stimulated emission process of an optical amplifier such as EDFA, there are some unaccounted channels of excitation energy losses in erbium active medium. One of these energy loss channels may be ESA of Er^{3+} on the emission wavelength at high excitation. For an EYDFA, a sharp decrease of quantum efficiency of luminescence sensitization of Er^{3+} by Yb^{3+} could be caused by this additional excitation energy losses during the laser operation[11]. The ESA process causes the excitation decay or upconversion luminescence. This fluorescence corresponds to a radiative transition from higher state to its neighboring level of lower energy[12,13].

2.3.3 Noise Characteristics

The noise characteristics are of importance in optical communication systems since they represent a major parameter that determines the overall system performance such as maximum transmission distance and bit rate.

Optical amplification, whether in fiber or semiconductor laser devices, introduces extra noise components into transmission systems due to contributions arising primarily from the ASE. Noise is generated when the optical signal is detected with ASE at an avalanche photo diode (APD) or p-i-n photodiode. The noise at the output terminal of an optical amplifier consists of the following five components[14,15]:

(i) signal-spontaneous beat noise

(ii) spontaneous-spontaneous beat noise

(iii) signal shot noise

(iv) spontaneous shot noise

(v) multiple path interference noise

These noises are referred as intensity/photocurrent noise. This noise refers to the power or current fluctuations associated with the optical beam. The two beat noises and interference noise are considered as excess noise. It is important to differentiate between shot noise and the excess noise since the resulting photocurrent noise they generate in an optical detector depends differently on the responsivity of the photodetector.

(i) signal-spontaneous noise:

This noise is due to interference between the signal light and ASE components where the signal and ASE fields must be in the same state of

polarization. Since the ASE is typically unpolarized, only one-half will contribute to the signal-spontaneous beat noise density. This noise is dominant in optical amplifier system.

$$N_{sig-sp} = \frac{P_{ASE}}{h\upsilon_s G \Delta\upsilon_s} \tag{2.16}$$

(ii) Spontaneous-spontaneous beat noise:

This noise is due to ASE heterodyning with itself, in other words, beating or mixing on an optical detector of the ASE continuum with itself. Their respective beat frequencies become higher if the mixing ASE wavelength components are spaced further apart. Fig.8 displays the two sources of beat noise in an optical amplifier.

$$N_{sp-sp} = \frac{P_{ASE}^2}{2h\upsilon_s G^2 P_s^{in} \Delta\upsilon_s} \tag{2.17}$$

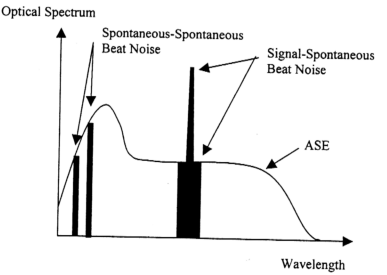

Fig.8 The signal-spontaneous beat noise and spontaneous-spontaneous beat noise generated in an optical amplifier.

(iii) & (iv) Signal shot noise and spontaneous shot noise:

Shot noise has its origins in the uncertainty of the time of arrival of electrons or photons at a detector. There is an electron-hole recombination process, which emits light in discrete in nature. In other words, there is randomness in the physical process where a photon is converted into an electron-hole pair, and there is uncertainty in the photon location, momentum, energy or arrival time.

The signal shot noise is due to the multiplication of the input power by the amplifier gain, whereas the spontaneous shot noise is caused by the integrated ASE power.

$$N_{sig,shot} = \frac{1}{G} \tag{2.18}$$

$$N_{sp,shot} = \frac{P_{ASE}}{G^2 P_s^{in}} \tag{2.19}$$

(v) Multiple path interference (MPI) noise:

Optical interference noise is due to the interference between the directly transmitted signal and the signals which are doubly reflected by the amplifier's internal reflection points.

$$N_{MPI} = \frac{2P_s^{in}}{h\upsilon\pi} \frac{\Delta\upsilon_s}{f^2 + \Delta\upsilon_s^2} \sum (P_i G_{cav,i}) \tag{2.20}$$

where $G_{cav,i}$ is cavity gain which is the gain in the i^{th} parasitic cavity inside the optical fiber amplifier. In other words, it is the gain in forward direction x reflectivity in forward direction x the gain in backward direction x reflectivity in backward direction; P_i is the polarization alignment factor which

expresses the matching of polarization states between the direct signal and the doubly reflected signal in the i^{th} cavity, $0 < P < 1$, P=1 for perfect alignment, so $P_i G_{cav,i}$ is the effective cavity gain in the i^{th} cavity and the sum is meant to collect all possible cavity gains in the optical amplifier, $\Delta\upsilon$ is the FWHM of the source linewidth (Lorentzian model) and f is the baseband frequency.

Thus, the total noise factor generated by the optical amplifier is

$$N_{total} = N_{sig\text{-}sp} + N_{sp\text{-}sp} + N_{sig,shot} + N_{sp,shot} + N_{MPI} \tag{2.21}$$

In the calculation of the noise factor of an optical amplifier, some assumptions are made as followed:

(1) the noise of the signal source is limited by quantum noise, i.e. the contribution from source relative intensity noise(RIN) is negligible;

(2) the photodetector noise is limited by shot noise, i.e. the contribution from thermal noise is negligible;

(3) the photodetector has a quantum efficiency of 1, so that the noise factor does not depend on the characteristics of the detector.

The amplifier optical noise figure is defined as

$$NF = \frac{SNR_{in}}{SNR_{out}} \tag{2.22}$$

The optical noise figure represents a measure of the SNR degradation experienced by the signal after passing through the amplifier. The SNRs are referred to the output of an ideal photodetector which is capable of converting

each photon of incident light into electrical current, that means in 100% quantum efficiency.

After all, the quantum-beat-noise-limited noise figure or the signal-spontaneous beat-noise-limited noise figure, which excludes the output SNR due to sp-sp beat noise, ASE shot noise, or MPI noise, is commonly used and derived as

$$NF = \frac{P_{ASE}}{h\upsilon G\Delta\upsilon} + \frac{1}{G} \tag{2.23}$$

where the first term in the right hand side of the above equation is the signal-spontaneous beat noise and the second term is the signal shot noise.

2.3.4 Applications of Optical Amplifiers

Optical amplifiers can serve several purposes in designing fiber-optic communication system. These are some possible applications of optical amplifiers:

(a) Power amplifier or power booster:

Optical amplifier can be used to increase the transmitted power by placing it just after the transmitter. A power amplifier increases the transmission distance by 10-100km depending on the amplifier gain and the fiber loss. Power amplifier is required to have a good saturation performance, as the input signal level to the amplifier will be relatively high (typically of the order of 1mW or 0dBm).

(b) Preamplifier:

Optical amplifier is placed directly in front of a receiver. This amplifier is used to amplify signals that may be below the sensitivity limit of a receiver. The output from the amplifier consists of the amplified signal and also a certain amount of ASE. Since the input signal power to the amplifier will be small, the total power due to ASE can be a substantial proportion of (or even more than) the amplified signal power. This ASE is normally spread over a much broader spectrum than the signal, thus the use of narrow band, low-loss optical filters can reject most of ASE, which could otherwise dramatically reduce the sensitivity of the receiver. It is possible to use two preamplifiers in series and receiver sensitivity will be improved. The preamplification of the optical signal makes it strong enough that thermal noise becomes negligible compared with shot noise.

(c) In-line amplifier:

In-line amplifiers are used especially in long-haul telecommunication systems to replace electronic regenerators. Electronic regeneration requires demultiplexing of channels before each channel signal is regenerated using separate receiver and transmitters, a rather costly procedure. On the other hand, optical amplifiers can amplify all channels simultaneously as long as their combined spectra lie within the amplifier bandwidth.

(d) Optical switch:

All types of optical amplifier require the supply of electrical current to a laser device to drive the amplification mechanism. Removal of this bias not

only removes the optical gain when the amplifier becomes strongly absorbing but, in some cases, the amplifier becomes opaque to the signal wavelengths. Hence, such a device can be used as an electrically controlled optical switch. However, these different optical amplifier switches have different response times.

2.4 Model of Er^{3+}/Yb^{3+} Codoped Fiber Amplifier

The Er^{3+}/Yb^{3+} glass laser has been studied and reported in [16]. By transferring energy from Yb^{3+} to Er^{3+} in a silicate glass, Er^{3+} has been made to emit laser oscillations at 1.54μm. The coupled Er^{3+}/Yb^{3+} system has been modeled through propagation-rate equations of a multilevel system by F.D.Pasquale[17-19]. The theoretical analysis of the dynamic behavior of Er^{3+}/Yb^{3+} system is described in [20]. Such analysis of dynamic behavior is particularly useful to avoid some effects such as self-pulsed behavior due to the presence of erbium ion-pairs[21]. Here, the theoretical model is described by the following steady-state rate equations and the conservation laws.

$$\frac{\partial n_1}{\partial t} = -W_{12}n_1 - W_{13}n_1 + A_{21}n_2 + W_{21}n_2 + C_{up}n_2^2 - C_{cr14}n_1n_4 + C_{up}n_3^2 + C_{cr}n_1n_6 = 0 \tag{2.24}$$

$$\frac{\partial n_2}{\partial t} = W_{12}n_1 - A_{21}n_2 - W_{21}n_2 + A_{32}n_3 - 2C_{up}n_2^2 + 2C_{cr14}n_1n_4 = 0 \tag{2.25}$$

$$\frac{\partial n_3}{\partial t} = W_{13}n_1 - A_{32}n_3 + A_{43}n_4 - 2C_{up}n_3^2 + C_{cr}n_1n_6 = 0 \tag{2.26}$$

$$n_1+n_2+n_3+n_4 = N_{Er} \tag{2.27}$$

$$\frac{\partial n_5}{\partial t} = -W_{56}n_5 + A_{65}n_6 + W_{65}n_6 + C_{cr}n_1n_6 = 0 \tag{2.28}$$

$$n_5 + n_6 = N_{Yb} \tag{2.29}$$

where n_1, n_2, n_3, n_4 represent the populations of Er^{3+} levels $^4I_{15/2}$, $^4I_{13/2}$, $^4I_{11/2}$, $^4I_{9/2}$ and n_5, n_6 are the populations of Yb^{3+} levels $^2F_{7/2}$ and $^2F_{5/2}$ respectively. Owing to the short lifetime of the $^4I_{11/2}$ pump Er^{3+} level, the back transfer of energy from Er^{3+} to Yb^{3+} has been neglected.

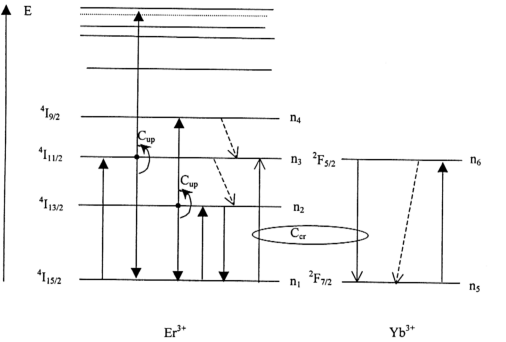

Fig.9 Schematic diagram of the relevant energy levels for the Er^{3+}/Yb^{3+} system.

Fig.9 shows the relevant energy levels for the coupled Er^{3+}/Yb^{3+} system. The W_{ij} terms represent stimulated transition rates; A_{21}, A_{65} are spontaneous transition rates; and A_{32}, A_{43} are nonradiative relaxation rates. As the preferred channel for energy transfer in the Er^{3+}/Yb^{3+} clusters occurs where

an excited electron in Yb^{3+} gives its energy to an electron in the ground state of Er^{3+}, the transfer of energy among neighbouring Yb^{3+} ions is neglected.

The uniform upconversion mechanisms from the Er^{3+} metastable and pump levels are modeled by quadratic terms in n_2 and n_3, with a concentration-dependent upconversion coefficient C_{up}; the pair-induced energy transfer process from Yb^{3+} to Er^{3+} is instead described by a constant cross-relaxation coefficient C_{cr}. The Er^{3+} ions are assumed to be homogeneously excited. This implies that they experience similar surroundings, and that the cooperative upconversion rate from the metastable level is homogeneous. Alternatively, the Er^{3+} concentration may be large enough to allow rapid energy migration in the acceptor sub-system. The energy migration rate in Er^{3+} can be expected to be higher than the cooperative upconversion rate due to the poor spectral overlap for cooperative upconversion. Thus, the upconversion may saturate in the kinetic limit. Therefore, homogeneous upconversion is modeled by a relaxation term quadratic in the concentration of excited Er^{3+}, with a concentration-independent upconversion coefficient. Homogeneous upconversion can be considered an ideal situation. It is also possible that the Er^{3+} distribution is inhomogeneous, with Er^{3+} ion clusters. These will act as quenching centers where rapid upconversion occurs.

The concentration-dependent upconversion coefficient C_{up} is assumed to be an increasing linear function of N_{Er}. For $N_{Er} = 4.4 \times 10^{25}$ ions/m^3, $C_{up} = 3.5 \times 10^{-24}$ m^3/sec; $N_{Er} = 1. \times 10^{26}$ ions/m^3, $C_{up} = 1.7 \times 10^{-23}$ m^3/sec. Under the assumption of dipole-dipole interactions, C_{up} can be expressed as:

$$C_{up} = \frac{4\pi}{3} \frac{R_0^6}{R_{Er/Er}^3 * \tau_{21}} \tag{2.30}$$

where $R_{Er/Er}$ is the average separation between uniformly distributed erbium ions; R_0 is a critical interaction distance; and $\tau_{21} = \frac{1}{A_{21}}$ is the lifetime of the $^4I_{13/2}$ erbium level.

The cross relaxation coefficient C_{cr} is estimated using the Forster-Dexter energy transfer model[22]. It is noted that C_{cr} has been considered to be of the same order as C_{up}.

$$C_{cr} = \frac{4\pi}{3} \frac{R_0^6}{R_{Yb/Er}^3 * \tau_{65}} \tag{2.31}$$

where $R_{Yb/Er}$ is the average distance between Yb^{3+} and Er^{3+} ions.

By assuming uniform spatial field distributions across the fiber core, the propagation equations for the pump power $P_p(z, \upsilon_p)$ and amplified spontaneous emission powers $P_{sj}^{\pm}(z, \upsilon_j)$ in an Er^{3+}/Yb^{3+} system can be written as followed[17]:

$$\frac{dP_p(z,\upsilon_p)}{dz} = -\Gamma_p[\sigma_{Er13} n_1 + \sigma_{Yb56} n_5 - \sigma_{Yb65} n_6] \times P_p(z,\upsilon_p) - l_p P_p(z,\upsilon_p) \tag{2.32}$$

$$\frac{dP_{sj}^{\pm}(z,\upsilon_j)}{dz} = \pm \Gamma_{sj}[\sigma_{Er21}(\upsilon_j) n_2 + \sigma_{Er12}(\upsilon_j) n_1] P_{sj}^{\pm}(z,\upsilon_j) \pm 2h\upsilon_j \Delta\upsilon_j \Gamma_{sj} \sigma_{Er21}(\upsilon_j) n_2 \mp l_{sj} P_{sj}^{\pm}(z,\upsilon_j) \tag{2.33}$$

where l_p and l_{sj} are the background losses; σ_{ij} and σ_{ji} are the absorption and emission cross sections; Γ_p and Γ_{sj} represent overlap integrals between the normalized field intensities and the active region[23]; and n_i is the average population densities corresponding to uniform spatial field distributions.

Pump light is absorbed by Yb^{3+} in the ground state ($^2F_{7/2}$) which is then excited to the $^2F_{5/2}$ state. Excited Yb^{3+} ions (donors) transfer energy to nearby ground state Er^{3+} ions (acceptors), whereby the Er^{3+} becomes excited to the pump level $^4I_{11/2}$. Since the lifetime of this level is short, it leads to a rapid relaxation to the metastable level $^4I_{13/2}$. Therefore, this prevents back transfer from Er^{3+} to Yb^{3+}.

Efficient pumping by Yb^{3+} sensitization may be used to improve amplification in EDFA, where the high Er^{3+} concentration will cause concentration quenching. This concentration quenching is due to the uniform and ion-pair upconversions, which deplete the Er^{3+} metastable level, and results in a serious pump-efficiency reduction. Therefore, there are some advantages using Yb^{3+}-sensitized EDFA. The Yb^{3+} sensitization extends the range of possible pump wavelengths from 800nm to 1100nm. It also lowers the local threshold power, P_{th} (the pump power that makes an infinitesimally short fiber transparent of the amplifier), so that even more pump power can be absorbed and an even higher inversion is obtained.

Yb^{3+} has three properties that qualify it as a useful co-dopant for Er^{3+}:

(1) The energy level of Yb^{3+} is simple. Yb^{3+} has only two energy manifolds (which ensures that no upconversion between ytterbium ions takes place),

and the excited level $^2F_{5/2}$ can transfer energy with good efficiency to the $^4I_{11/2}$ level of Er^{3+};

(2) The ionic radius of Yb^{3+} is not so different from that of Er^{3+} (refer back to Table 2), making it possible to surround each Er^{3+} ion with several Yb^{3+} ions in order to facilitate an efficient energy transfer;

(3) Similar to Er^{3+}, Yb^{3+} also tends to cluster with one erbium surrounded by several ytterbium ions. These features have the effect of both increasing the efficiency of energy transfer from Yb^{3+} to Er^{3+} and of reducing upconversion among Er^{3+} ions to the level expected in a uniform Er^{3+} ion distribution.

However, if N_{Yb}/N_{Er} ratio is too high, the formation of ytterbium clusters and quenching happens, this quenching centers will be extremely harmful: efficient pumping of quenching centers will result in an efficient drain for the pump light, pump energy will be wasted and consequently reduce amplifier efficiency. Therefore the advantage of Yb^{3+} sensitization may vanish. Besides, scattering losses caused by Yb^{3+} ions may also degrade the EYDFA.

Reference:

[1] Shoichi Sudo, "Optical Fiber Amplifiers: Material, Devices, and Applications," Artech House,Inc. 1997.

[2] E.Snitzer, "Glass Lasers," Appl. Optics., vol.5, no.10, pp.1487-1499, 1966.

[3] E.Snitzer, and K.Wei, "Materials Considerations for Fiber Amplifiers," FP1.1 , Rutgers University Piscataway, New Jersey.

[4] M.P.Petrov, R.V.Kiyan, E.A.Kuzin, E.A.Rogacheva, and V.V.Spirin, "Gain saaturation in three- and four-level fiber amplifiers," Optics Comm., 109, pp. 499-506, July 1994.

[5] J.R.Armitage, "Three-level fiber laser amplifier," Appl. Optics., vol.27, no.23, 1988.

[6] M.J.F.Digonnet, "Theory of Operation of Three- and Four-Level Amplifiers and Sources," SPIE, vol.1171, 1989.

[7] Emmanuel Desurvire, "Erbium-doped Fiber Amplifiers," John Wiley & Sons, Inc. 1994.

[8] Dennis Derickson, "Fiber Optic Test and Measurement," Hewlett-Packard Company, 1998.

[9] W.M.Fairbank Jr., G.K.Klauminzer and A.L.Schawlow, Phys.Rev. B, 11,60, 1975.

[10] C.G.Atkins, J.R.Armitage, R.Wyatt, B.J. Ainslie and S.P. Craig-Ryan, "Pump Excited State Absorption in Er^{3+} Doped Optical Fibers," Optics Comm., vol.73, no.3, Oct. 1989.

[11] V.P.Gapontsev, S.M. Matitsin, and A.A. Isineev, "Channels of Energy Losses in Erbium Laser Glasses in the Stimulated Emission Process," Optics Comm., vol.46, no.3.4, July 1983.

[12] J.P.Wittke, I.Ladany, and P.N.Yocom, "Y_2O_3:Yb:Er-New Red-Emitting nfrared-Excited Phosphor, " J.Appl.Phys., vol.43, no.2, Feb.1972.

[13] Yi-Min Hua *et al*, "Frequency upconversion in Er^{3+} and Yb^{3+}/Er^{3+}-doped silica fibers, " Optics Comm., 88, pp.441-445, 1992.

[14] "OFA Noise Figure – The Mathematical Model," Hewlett Packard, 1995.

[15] P.R.Morkel, R.I.Laming, G.J.Cowle, and D.N.Payne, "Noise characteristics of rare-earth-doped fiber sources and amplifiers," Optoelectronics Research Centre, University of Southampton.

[16] E.Snitzer, and R.Woodcock, "Yb^{3+}-Er^{3+} Glass Laser," Appl. Phys. Lett., vol.6, no.3, 1965.

[17] F.D.Pasquale, "Modeling of Highly-Efficient Grating-Feedback and Fabry-Perot Er^{3+}-Yb^{3+} Co-Doped Fiber Lasers," IEEE J.Quan.Electro., vol.32, no.2, 1996.

[18] F.D.Pasquale, and M.Federighi, "Improved Gain Characteristics in High-Concentration Er^{3+}/Yb^{3+} Codoped Glass Waveguide Amplifiers," IEEE J.Quan.Electro., vol.30, no.9, 1994.

[19] M.Federighi, and F.D.Pasquale, "The Effect of Pair-Induced Energy Transfer on the Performance of Silica Waveguide Amplifiers with High Er^{3+}/Yb^{3+} Concentrations," IEEE Photonics Tech. Lett., vol.7, no.3, 1995.

[20] T.Tellert, F.D. Pasquale, and M.Federighi, "Theoretical Analysis of the Dynamic Behavior of Highly-Efficient Erbium/Ytterbium Codoped Fiber Lasers," IEEE Photonics Tech. Lett., vol.8, no.11, 1996.

[21] F. Sanchez, P.Le Boudec, and G.Stephan, "Effects of ion pairs on the dynamics of erbium-doped fiber lasers," Phys.Rev. A, vol.48, no.3, 1993.

[22] W.Q.Shi, M. Bass, and M. Bimbaum, "Effects of energy transfer among Er^{3+} ions on the fluorescence decay and lasing properties of heavily doped Er:$Y_3Al_5O_{12}$," J. Opt. Soc. Am. B, vol.7, no.8, pp.1456-1462, 1990.

[23] E.Desurvire, and J.R.Simpson, "Amplification of spontaneous emission in erbium-doped single-mode fibers," J.Lightwave Technol., vol.7, no.5, 1989.